

An optimization-based “phase field” model for polycrystalline ferroelectrics

F. X. Li,^{1,2,a)} X. L. Zhou,¹ and A. K. Soh^{3,b)}

¹State Key Laboratory for Turbulence and Complex Systems, College of Engineering, Peking University, Beijing 100871, China

²Center for Applied Physics and Technology, Peking University, Beijing 100871, China

³Department of Mechanical Engineering, The University of Hong Kong, Hong Kong Special Administrative Region, China

(Received 10 January 2010; accepted 11 March 2010; published online 13 April 2010)

An optimization-based computational model is proposed to study domain evolution in polycrystalline ferroelectrics composed of numerous grains, each of which consists of multiple domains. Domain switching is realized by an optimization process to minimize the free energy of each grain. Similar to phase field modeling, no *priori* domain-switching criterion is imposed in the proposed model. Moreover, by focusing on the volume fractions of domains only, the computational complexity of this model becomes much smaller and the domain textures evolution can be captured. Simulation results on both tetragonal and rhombohedral lead titanate zirconate ceramics illustrate the efficiency of this model. © 2010 American Institute of Physics. [doi:10.1063/1.3377899]

Ferroelectric materials have been widely used in modern industries as sensors, actuators, transducers, etc. This type of materials shows excellent linear response at low electric/stress fields but exhibits significant nonlinearities under a large electric field or high stress due to domain switching.¹ Modeling of domain switching in ferroelectric materials has received intensive attentions in recent years,^{2–11} among which the phase field model (PFM) seems more promising.^{6–11} No imposition of any *priori* domain-switching criterion is required in PFM, and domain switching is a natural process during minimization of the whole material system's total free energy. Although PFM has achieved great success in modeling domain evolutions in ferroelectric single crystals, it has hardly been used for modeling polycrystalline ferroelectrics.^{9–11} In our recent works,¹² domain switching problems in polycrystalline ferroelectrics have been addressed by an analytical constrained domain-switching model, in which a *priori* domain-switching criterion must be prescribed and only uniaxial loading is allowed to determine the analytical solution. Thus, it is not suitable for a general computational study of domain evolution in polycrystalline ferroelectrics under arbitrary loading. In this letter, we propose an optimization-based computational model to study domain switching in polycrystalline ferroelectrics. Similar to PFM, no *priori* domain-switching criterion is imposed in the proposed model, whose computational complexity is, however, much smaller than that of PFM and, therefore, it is able to handle three-dimensional (3D) cases where numerous grains are modeled. Moreover, the domain texture evolution process under applied loading can be illustrated.

In the present model, a polycrystalline ferroelectric is made up of numerous randomly oriented grains each of which contains N types of domains (where $N=6$ for the tetragonal case and $N=8$ for the rhombohedral case, etc.), the volume fraction of each type of domains is denoted by f_i ($i=1, 2, \dots, N$) and $\sum_{i=1}^N f_i=1$. Both the electric and elastic interactions between grains are considered in a self-consistent inclusion manner.¹³ In other words, each grain is regarded as

an inclusion surrounded by an infinite large matrix with the materials properties same as the whole material, as shown in Fig. 1, which is two-dimensional. As spherical shape is the simplest one and no other shapes are more appropriate, such shape is employed for modeling of inclusions. Moreover, by adopting the concept of Eshelby's inclusion,¹³ both the electric and stress fields are assumed to be uniform inside each grain (inclusion), i.e., the interactions between domains in the same grain are neglected. Furthermore, in order to account for the major characteristics of domain switching and to make computation manageable, a polycrystalline ferroelectric is assumed to exhibit dielectric and elastic isotropy and shows linear dielectric and elastic behavior unless domain switching occurs.

In the conventional PFM, the free energy of the whole material system subjected to external loading is minimized using the time-dependent Ginzburg–Landau equation to determine the final stabilized domain structures. As the computational complexity of this minimization process increases drastically with increasing number of computing grids,⁶ PFM is usually used to simulate two-dimensional (2D) single crystals. In the present model, to make the computational complexity manageable in 3D case, the focus is not placed on the energy minimization process but only on the final stabilized state. Besides, as the interactions between grains have been considered in an Eshelby inclusion manner in this model, the free energy of each grain is used as the optimization objective and the optimization process is carried out for all grains to determine the domain structures and properties of the whole material system. The free energy of a specific grain can be expressed as

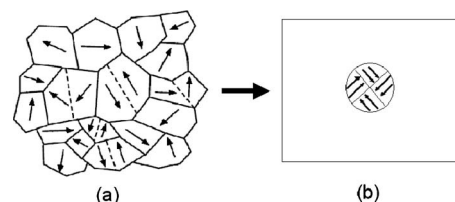


FIG. 1. 2D Illustration of material model for polycrystalline ferroelectrics.

^{a)}Electronic mail: lifaxin@pku.edu.cn. Tel.: 86 10 62757454. FAX: 86 10 62751812.

^{b)}Electronic mail: aksoh@hku.hk. Tel.: 852 28598061.

TABLE I. Material constants of tetragonal and rhombohedral PZT used in the model.

| Material constants | Rhombohedral | Tetragonal |
|--|----------------------|----------------------|
| Shear modulus μ (GPa) | 30 | 30 |
| Poisson's ratio ν | 0.3 | 0.3 |
| Dielectric constant k (F/m) | 1.0×10^{-8} | 1.0×10^{-8} |
| Spontaneous polarization P_0 (C/m ²) | 0.52 | 0.52 |
| Lattice deformation S_{lattice} | 0.65% | 2.77% |
| Coercive field E_C (kV/mm) | 1.0 | 1.0 |

$$\begin{aligned}
U(\mathbf{E}, \boldsymbol{\sigma}) = & -\mathbf{E} \cdot \mathbf{P}^r - \boldsymbol{\sigma} : \boldsymbol{\epsilon}^r + \frac{1}{2} k \mathbf{E} \cdot \mathbf{E} + \frac{1}{2} \frac{1}{2\mu} \boldsymbol{\sigma} : \boldsymbol{\sigma} \\
& - \frac{1}{2} \frac{\nu}{2\mu(1+\nu)} [\text{tr}(\boldsymbol{\sigma})]^2 + \frac{1}{2} \frac{7-5\nu}{2\mu(1-\nu^2)} (\boldsymbol{\epsilon}^r \\
& - \bar{\boldsymbol{\epsilon}}) : (\boldsymbol{\epsilon}^r - \bar{\boldsymbol{\epsilon}}) + \frac{1}{2} \times L \frac{1}{3k} (\mathbf{P}^r - \bar{\mathbf{P}}^r) \cdot (\mathbf{P}^r - \bar{\mathbf{P}}^r) \\
& + f_{180} W_{180} + f_{\text{non-180}} W_{\text{non-180}}, \quad (1)
\end{aligned}$$

where \mathbf{E} , $\boldsymbol{\sigma}$ are the applied electric field tensor, and applied stress tensor, respectively; k is the isotropic dielectric constant; μ, ν denote the isotropic shear modulus and Poisson's ratio, respectively; $\bar{\boldsymbol{\epsilon}}$, $\bar{\mathbf{P}}^r$ are the average strain and polarization of the whole material system or the matrix, respectively; L ($0 \leq L \leq 1$) is the electric depolarization factor, which depends on the extent of charge screening;¹⁴ \mathbf{P}^r and $\boldsymbol{\epsilon}^r$ are the remnant polarization and remnant strain of a grain, which can be expressed as linear functions of the volume fractions of domains as follows:

$$\mathbf{P}^r = \sum_{i=1}^N f_i \mathbf{P}^i, \quad \boldsymbol{\epsilon}^r = \sum_{i=1}^N f_i \boldsymbol{\epsilon}^i, \quad (2)$$

where \mathbf{P}^i and $\boldsymbol{\epsilon}^i$ are the spontaneous polarization and spontaneous strain tensor of the i th domain.

W_{180} and $W_{\text{non-180}}$ are the energy barrier (per unit volume) for 180° and non-180° domain switching, respectively; and f_{180} and $f_{\text{non-180}}$ are the corresponding volume fractions, which can be calculated as follows:

$$f_{\text{non-180}} = \frac{1}{2} \sum_{i=1}^{N/2} |f_{2i-1} + f_{2i} - (f_{2i-1}^0 + f_{2i-1}^0)|, \quad (3a)$$

$$f_{180} = \frac{1}{2} \sum_{i=1}^N |f_i - f_i^0| - f_{\text{non-180}}, \quad (3b)$$

where f_i^0 is the volume fraction of the i th domain calculated at last loading step.

Referring to the expression of the free energy given in Eq. (1), the first two items on the right hand side is the potential energy;¹ the third item is the linear dielectric energy, the fourth and fifth items present the linear strain energy; the sixth and seventh items are the elastic and electric inclusion energies, respectively; and the last two items are the dissipation energies during domain switching, which are similar to the domain wall energy in the conventional PFM.⁶

The volume fractions of domains, i.e., the optimization variables, at a specific loading are obtained by minimizing the total free energy of each of the grains in a ferroelectric

polycrystalline. The mathematical optimization problem for this model can be summarized by the following:

Problem I

$$\text{Min } U(f_1, f_2, \dots, f_N),$$

$$s.t. \quad 0 \leq f_i \leq 1 \quad (i = 1, 2, \dots, N),$$

$$\sum_{i=1}^N f_i = 1.$$

As the free energy is a nonlinear function of the volume fractions of domains, **Problem I** becomes a constrained nonlinear optimization problem. To solve this type of optimization problems, the sequential quadratic programming method¹⁵ is a very effective algorithm with high accuracy and quick convergence. As the expression of the free energy varies from grain to grain and depends on the applied loading, at each loading step, the optimization process involves all grains to determine the domain structures, polarizations, and strains.

The behavior of both tetragonal and rhombohedral PZT ferroelectric ceramics under cyclic electric loading are studied using the proposed optimization model consisting of 10 000 grains, in which the charge screening that exists in real ceramics^{12,16} is taken into account. Thus, the depolarization field induced by polarization switching vanishes, i.e., $L=0$ in Eq. (1). The material constants used are listed in Table I, which are taken from Hoffmann *et al.*¹⁷ but with

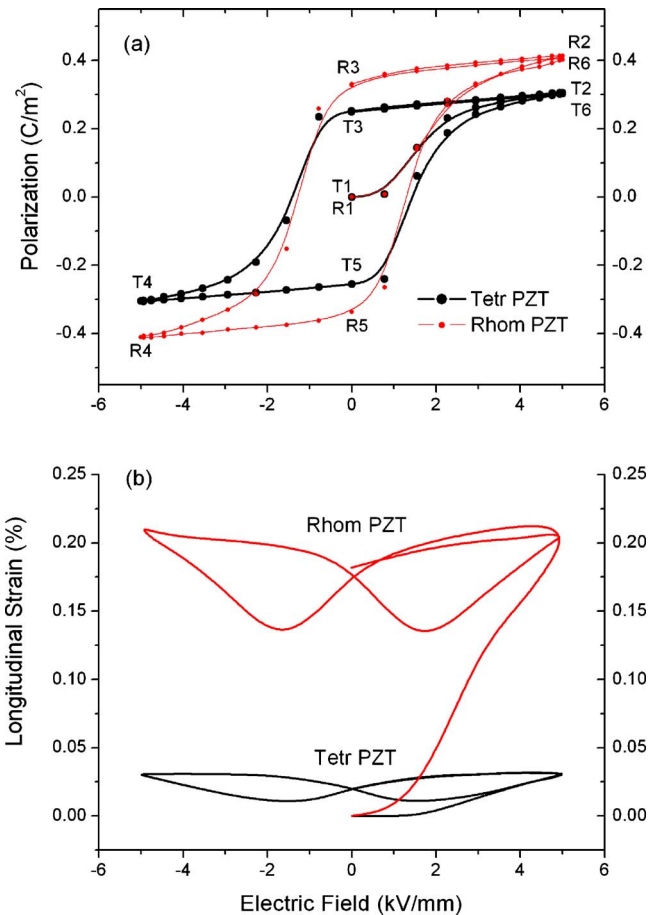


FIG. 2. (Color online) Simulated (a) polarization and (b) strain curves of tetragonal and rhombohedral PZT ceramics under applied electric loading.

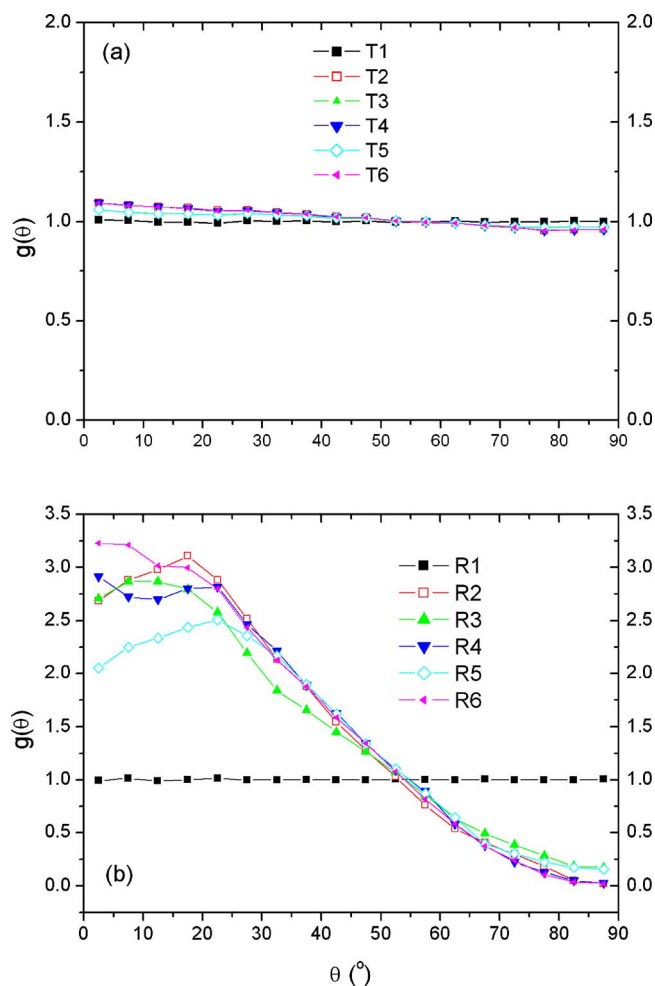


FIG. 3. (Color online) Calculated (a) (001) pole figures in tetragonal PZT ceramics and (b) (111) pole figures in rhombohedral PZT ceramics corresponding to different electric loading points in Fig. 2(a).

slight modifications because of the isotropic dielectric and elastic assumptions. For easy comparison, the elastic and dielectric properties, spontaneous polarization, and the nominal coercive field of these two types of ceramics are taken to be the same as they do not differ much in reality. Note that in Table I, the lattice deformation $S_{\text{lattice}} = c/a - 1$ and $S_{\text{lattice}} = d_{[111]}/d_{[111]} - 1$ for the tetragonal and rhombohedral types, respectively.¹² In addition, the energy barriers for both 180° and non-180° switching are taken to be $2P_0E_C$.¹

Figure 2 shows the plots of calculated polarization and longitudinal strain under cyclic electric loading up to $5E_C$ for both tetragonal and rhombohedral PZT ceramics. The curves overlap themselves very well during cyclic loading which confirms good convergence of this model. The computation time required on a Pentium 3.0 GHz PC for 61 loading steps is about 7 h for the tetragonal PZT and about 12 h for the rhombohedral PZT, and it increases only linearly with increasing number of grains. In Fig. 2, both the remnant polarization and strain of the rhombohedral PZT ceramics are obviously larger than those of the tetragonal PZT ceramics, which are consistent with previous experiments¹⁷ and predictions.¹² The rather flat strain curve of the tetragonal ceramics indicates that little 90° domain switching has occurred, even though the 180° switching is almost complete, which can be estimated from the polarization curve in Fig. 2(a). The large remnant strain of rhombohedral PZT ceram-

ics shows that considerable amount of non-180° switching has occurred during electric poling.

The evolution process of the domain textures (represented by the pole figures of polar axes in this paper) can also be captured by this optimization model. Under electric loading or uni-axial compression (tension), the pole figure of polar axis is axisymmetric around the field direction and, thus, can be described by an angular distribution function $g(\theta)$ ($0 \leq \theta \leq \pi/2$).¹⁸ Note that $g(\theta) \equiv 1$ for a random uniform distribution and the normalization condition requires $\int_0^{\pi/2} g(\theta) \sin \theta d\theta = 1$. Obviously, $g(\theta)$ completely depends on non-180° domain switching. In this paper, $g(\theta)$ is calculated by dividing the interval of $[0, 90^\circ]$ into eighteen subintervals each of which is 5° . The accumulated volume fractions of domains at all these subintervals give rise to $g(\theta)$ at discrete values of θ .

Figure 3 shows the domain textures in both tetragonal and rhombohedral PZT ceramics corresponding to the electric loading points indicated in Fig. 2(a). It can be seen from Fig. 3(a) that during electric loading, the domain textures of tetragonal PZT ceramics change little from the initial unpoled state. This indicates that little 90° domain switching occurs which is consistent with the small remnant strain shown in Fig. 2(b). Whereas, the domain textures of rhombohedral PZT ceramics change a lot from the unpoled state during electric poling (R1 → R2), as shown in Fig. 3(b), which shows that upon removing the electric field, domain switching reverses causing domain texture variations (R2 → R3). Nevertheless, in rhombohedral PZT ceramics, the domain textures cannot return to the initial unpoled state in subsequent electric loading after poling.

F.L. gratefully thanks Professor X. Guo (Dalian University of Technology) for his helpful discussions. This work is supported by the Natural Science Foundation (Grant No. 10872002), the 985 Project Foundation of Peking University, and the Research Grants Council of the Hong Kong Special Administrative Region, China (Project No. HKU 716007E).

¹S. C. Hwang, C. S. Lynch, and R. M. McMeeking, *Acta Metall. Mater.* **43**, 2073 (1995).

²J. E. Huber, N. A. Fleck, C. M. Landis, and R. M. McMeeking, *J. Mech. Phys. Solids* **47**, 1663 (1999).

³C. M. Landis, *J. Mech. Phys. Solids* **50**, 127 (2002).

⁴F. X. Li and D. N. Fang, *Mech. Mater.* **36**, 959 (2004).

⁵W. Tang, D. N. Fang, and J. Y. Li, *J. Mech. Phys. Solids* **57**, 1683 (2009).

⁶L. Q. Chen, *Annu. Rev. Mater. Res.* **32**, 113 (2002).

⁷A. K. Soh, Y. C. Song, and Y. Ni, *J. Am. Ceram. Soc.* **89**, 652 (2006).

⁸J. Wang and M. Kamlah, *Appl. Phys. Lett.* **93**, 042906 (2008).

⁹Y. U. Wang, Y. M. Jin, and A. G. Khachaturyan, *J. Appl. Phys.* **92**, 1351 (2002).

¹⁰S. Choudhury, Y. L. Li, C. E. Krill III, and L. Q. Chen, *Acta Mater.* **53**, 5313 (2005).

¹¹D. Schrade, R. Mueller, B. Xu, and D. Gross, *Comput. Methods Appl. Mech. Eng.* **196**, 4365 (2007).

¹²F. X. Li and R. K. N. D. Rajapakse, *Acta Mater.* **55**, 6472 (2007); **55**, 6481 (2007).

¹³J. D. Eshelby, *Proc. R. Soc. London, Ser. A* **241**, 376 (1957).

¹⁴M. E. Lines and A. M. Glass, *Principles and Applications of Ferroelectrics and Related Materials* (Clarendon, Oxford, 1977), p. 87.

¹⁵S. P. Han, *J. Optim. Theory Appl.* **22**, 297 (1977).

¹⁶D. A. Hall, A. Steuwer, B. Cherdhirunkorn, P. J. Withers, and T. Mori, *J. Mech. Phys. Solids* **53**, 249 (2005).

¹⁷M. J. Hoffmann, M. Hamme, A. Endriss, and D. C. Lupascu, *Acta Mater.* **49**, 1301 (2001).

¹⁸F. X. Li and R. K. N. D. Rajapakse, *J. Appl. Phys.* **101**, 054110 (2007).